GEOPHYSICAL RESEARCH LETTERS, VOL. 24, NO.13, PAGES 1687-1690, JULY 1, 1997

JULIA radar studies of electric fields in the equatorial electrojet

D. L. Hysell and M. F. Larsen

Department of Physics and Astronomy, Clemson University, Clemson, South Carolina

R. F. Woodman

Instituto Geofísico del Perú, Lima

Abstract. First results from the JULIA radar at Jicamarca are presented. These include coherent scatter observations of the equatorial electrojet and of 150-km echoes. Interferometry is used to measure the zonal drift rate of kilometer scale waves in the electrojet as functions of altitude. A technique for estimating the background zonal electric field from the interferometry data is described. The electric field estimates can be calibrated against the Doppler speed of the 150-km echoes when the latter are present. The kilometer-scale wave drifts sometimes exhibit large-amplitude, periodic height variations with vertical wavelengths of about 10 km. These signatures are reminiscent of the wind profiles measured with chemical release techniques in the lower thermosphere during the Guará campaign.

Introduction

In this paper, we present the first observations of the JULIA radar located at the Jicamarca Radio Observatory near Lima, Perú. JULIA is an independent PC-based data acquisition system that makes use of the exciter stages of the Jicamarca radar along with the main antenna array. In many ways, this system duplicates the function of the Jicamarca radar except that it does not use the main high-power transmitters. With its pair of 30 kW peak power pulsed transmitters driving a $(290\ \mathrm{m})^2$ modular antenna array, JULIA is a formidable MST/coherent scatter radar. It is uniquely suited for studying the day-to-day and long-term variability of equatorial irregularities, which until now have only been investigated episodicly or in campaign mode.

This paper briefly presents three recent findings. First, it shows that the JULIA radar is sensitive enough to make high-quality observations of the equatorial electrojet and of the so-called "150-km echoes" from the valley region investigated by *Kudeki and Fawcett* [1993]. Second, it demonstrates the manner in which the zonal electric field can also be inferred from interferometric observations of km-scale waves in the equatorial electrojet. Third, it suggests that the electrodynamics in the electrojet may be strongly affected by the neutral atmospheric flow field and tidal structure and that JULIA may provide a means of monitoring that structure.

Paper number 97GL00373.
0094-8534/97/97GL-00373$05.00

JULIA Observations

The JULIA radar is configured to excite two 30 kW peak power 50 Mc transmitters generating pulse lengths up to about 15 μs with a 2% maximum duty cycle. For this experiment, one transmitter each is connected to the north and south quarters of the Jicamarca antenna array. Receivers are connected to the east and west quarters, providing a zonal interferometry baseline length of approximately 34 λ. Observations made in this configuration are described below.

150-km Echoes

Figure 1 presents examples of power and drift data collected by JULIA. It shows coherent scatter from the equatorial electrojet as well as so-called "150-km" echoes that are most visible around noon. These particular data were collected using a 1.5 km (10 μs) transmitter pulse, an inter-pulse period (IPP) of 187.5 km (1.25 ms), and with 10 coherent integrations. Grayscales de-

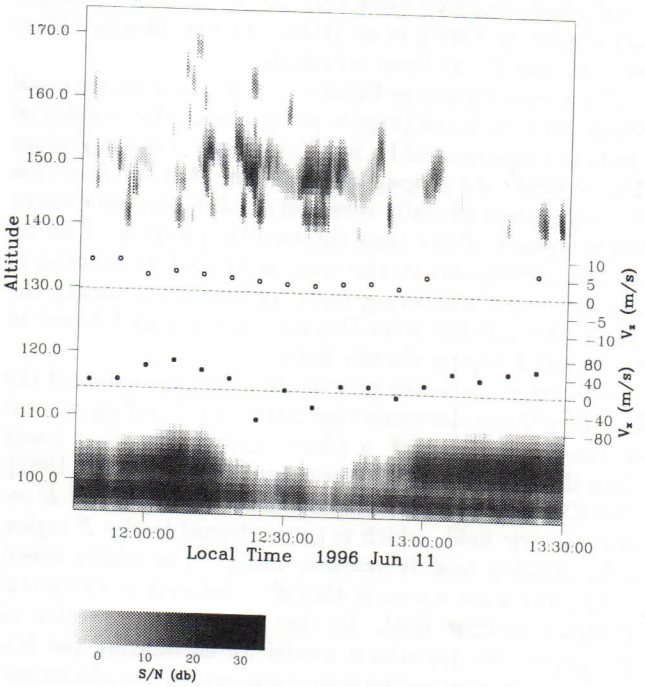

Figure 1. Range time intensity plot depicting backscatter from the electrojet along with 150-km echoes (see text).

pict signal-to-noise ratios computed using 16 s incoherent integrations. Note that coherent integration enhanced the detectability of the spectrally-narrow 150-km echoes but may well have rejected a significant portion of the broadband electrojet backscatter.

The open circles in Figure 1 are measurements of the vertical Doppler velocity V_z corresponding to the 150-km echo region. Positive values correspond to negative Doppler shifts and hence to upward motion. The measured values range between about 2 and 8 m/s with a pronounced dip occuring near the midpoint of the observations, when the 150-km echoes were strongest.

Kudeki and Fawcett [1993] showed that the phase velocities of the 150-km echoes are proportional to the electrojet current and argued that these velocities are indicative of the zonal electric field in the ionosphere. They pointed out that it might be possible to make electric field measurements in the ionosphere with a small Doppler radar by monitoring the 150-km echoes. Recently, *Woodman and Villanueva* [1995] verified via incoherent scatter experiments that the 150-km echo phase velocities are indeed good estimates of F region vertical plasma drifts. The Doppler speeds presented in Figure 1 therefore signify that the eastward F region zonal electric field ranged from about 0.05 to 0.2 mV/m during the time interval shown.

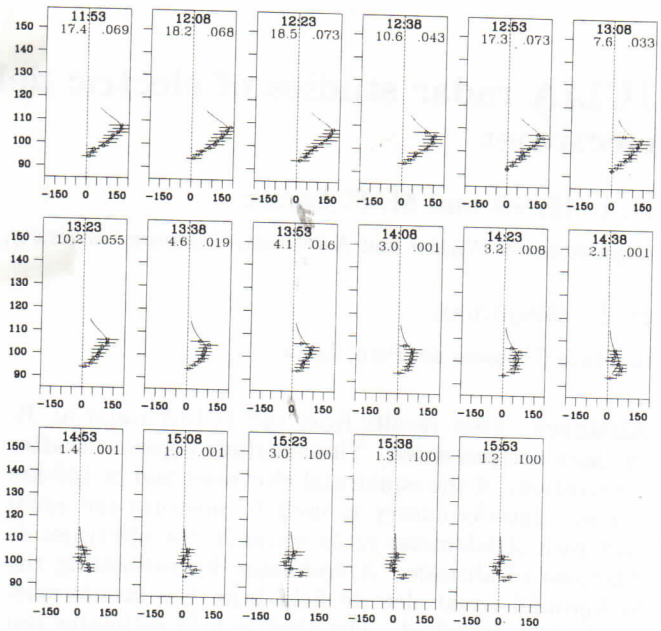

Figure 2. Zonal drift rates of km-scale waves on April 10, 1996. The vertical scales represent altitude in km, and the horizontal scales zonal phase speeds in m/s. Positive values denote westward propagation.

Zonal Drifts of Large Scale Electrojet Waves

Large-scale gradient drift waves in the electrojet with horizontal wavelengths near 1 km in the daytime generate enhanced radar backscatter from regions physically localized around their wave fronts [*Kudeki et al.*, 1982]. We can track the zonal progression of these wavefronts through the Jicamarca antenna beam and infer their zonal phase velocity using the interferometry technique introduced by *Farley et al.* [1981]. Our technique differs only in that it has been automated.

The closed circles in Figure 1 show the average zonal phase velocity V_x of large-scale waves in the equatorial electrojet determined by interferometry. Positive values denote westward propagation. We see that the direction of propagation actually reversed on three occasions near the midpoint of the time interval in question. The reversals correspond to the narrowing and weakening of the electrojet scattering layer and occured during the dip in the 150-km echo Doppler velocity and hence in the zonal F region electric field.

The km-scale waves propagate in the direction of the $\mathbf{E} \times \mathbf{B}$ drifting electrons that carry the Cowling current in the electrojet with a phase speed somewhat lower than the speed of the electron fluid [*Kudeki et al.*, 1982]. The Cowling current is established by the zonal E region electric field, which is proportional to the F region field [*Balsley and Woodman*, 1969]. The phase speed of the km-scale waves is therefore related to the zonal F region electric field. In the "Discussion" section of the paper, we describe a model for estimating the latter from interferometry measurements in the electrojet. Before getting to the model, however, we must examine the height variation of the km-scale wave phase speeds.

Figure 2 presents interferometry data from a quiescent electrojet layer observed on April 10, 1996 (this time without coherent integration). The data points in each frame correspond to the zonal phase velocity of km-scale waves observed at a given altitude and time (positive values denote westward propagation). Data points were averaged for approximately 15 minutes, and the lines through the points represent RMS variations in the data (not error bars). We see that the phase velocity profiles typically peak between 105–108 km and grow as large as 200 m/s.

The solid lines through the data points are model fits. Once again, we delay description of the model for the "Discussion" section of the paper and merely illustrate here that it seems to be able to reproduce the important features of the data, although there are significant discrepancies highlighted below. The pair of numbers written in each data frame are two parameters that fall out of the model fitting. The number at the upper left is the electric field parameter $\alpha E_o/B$, where E_o is the zonal F region electric field. The dimensionless α factor is approximately equal to 1/2, is weakly height and time dependent, and must be determined through some sort of calibration. The number to the right is the RMS turbulent intensity parameter, $\langle|\delta n/n|^2\rangle^{1/2}$, where δn is the density fluctuation associated with small-scale electrojet turbulence (see below).

If we pick α to be 2/3 in this case, then the zonal electric field predicted by the model fitting peaks at noon (at 0.7 mV/m or 28 m/s) and slowly declines to near zero at 1600 LT with values along the way that coincide fairly well with the seasonal average [*Fejer et al.*, 1979]. JULIA seems to be able to infer the F region zonal electric field from E region irregularity phase velocities, to within a "constant". The constant can be set either by adjustment to seasonal averages or by comparison to the 150-km echo Doppler speeds, the preferred technique.

Neutral Winds

As time progresses, the profiles in Figure 2 begin to look periodic and depart from the model curves, which are singly-peaked. The periodic structure is persistent, has a vertical wavelength of about 10 km, and shows a slow downward phase progression. The wave amplitude is about 40 m/s. Longer data sets, not shown here, obtained recently with the JULIA system indicate that the period associated with the propagating structure is approximately 12 hr.

Figure 3 is a more dramatic example of periodically-varying zonal drift profiles measured by the JULIA radar, this time on May 16, 1996. These curves illustrate the evening reversal of the zonal electric field, when the phase speed of gradient-drift waves reversed from westward to eastward around 1930 LT. However before about 2100 LT, the profiles are disturbed by a strong, downward propagating periodic variation with a vertical wavelength of about 10 km and an amplitude greater than 50 m/s.

Kudeki et al. [1987] saw a puzzling reversal in the direction of the km-scale wave drifts in their nighttime electrojet data. They attributed the reversal to neutral wind shear but were tentative because neutral wind speeds of the order of 100 m/s were required. Indeed, the various tidal models, such as the global-scale wind model *Hagan et al.* [1995] and *Forbes and Vial* [1989], do not predict winds or wind shears large enough to account for the observations. However, TMA experiments carried out at the magnetic equator in Brazil [*Larsen and Odom*, 1997] as part of the Guará rocket campaign show winds and shears of that magnitude in the 90 to 110 km altitude range on both days when chemical release wind measurements were carried out near sunset. Their zonal wind profiles have wavelike features with vertical wavelengths between 5 and 20 km and amplitudes of 50–80 m/s. E region wind measurements from Thumba carried out in 1975 by Rees and co-workers (described in the review article by *Forbes* [1981]) also showed small vertical scale sizes and wind speeds exceeding 100 m/s in the 90 to 110 km altitude range.

If wind shears and wind speeds of the right magnitude are present, as the chemical release observations seem to suggest, then they will modulate the plasma drifts and the currents as described theoretically by *Forbes and Lindzen* [1976], for example. The electrojet interferometry measurements thus appear to be able to detect the effects of these neutral wind fluctuations.

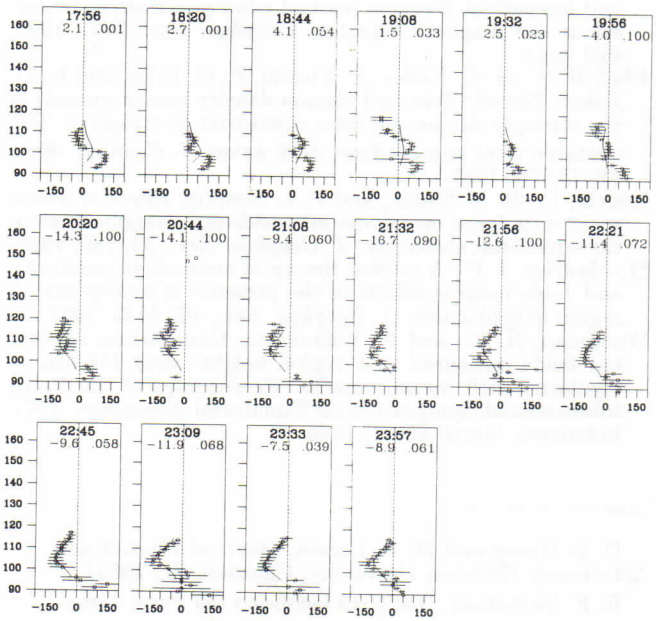

Figure 3. Similar to Figure 2 for May 16, 1996. This time, the curves exhibit large-amplitude periodic variations associated with neutral atmospheric waves.

Discussion

The linear theory for electrojet plasma waves has been investigated by numerous authors and leads to the following expression for the real part of the wave frequency:

$$\omega_r = \frac{\mathbf{k}\cdot\mathbf{V}_d}{1+\psi}\frac{1}{1+(k_o/k)^2} \qquad (1)$$

where $\psi = \nu_{in}\nu_e/\Omega_i\Omega_e$, k is the horizontal wavenumber, $k_o = \nu_{in}/\Omega_i L(1+\psi)^{-1}$, L is the plasma density gradient scale length, and where Ω_j and ν_j refer to the cyclotron and collision frequencies of species j respectively. The k_o/k term above becomes important for wavelengths comparable to the E region density gradient scale length [*Kudeki et al.*, 1982]. The term $\mathbf{V}_d$ above refers to the electron drift velocity, which is just their $\mathbf{E}\times\mathbf{B}$ drift velocity in the presence of the vertical polarization electric field in the electrojet. This polarization field (E_p) arises to maintain charge neutrality and can be related to the E region background zonal electric field (E_o) through the approximate expression

$$E_p(z) \approx E_o\sigma_H(z)/\sigma_P(z) \qquad (2)$$

where $\sigma_H(z)$ and $\sigma_P(z)$ are the E region Hall and Pedersen conductivities as functions of altitude. Combining (1) and (2) yields a simple relationship between the phase speed of horizontally propagating large-scale gradient drift waves $V(z)$ and the background zonal electric field:

$$\underbrace{V(z)}_{\text{data}} = \underbrace{\frac{\sigma_H(z)/\sigma_P(z)}{1+\psi(z)}}_{\text{model}}\underbrace{\frac{E_o/B}{1+(k_o/k)^2}}_{\text{E-field param.}} \qquad (3)$$

Equation (3) then gives a prescription for estimating the zonal electric field from km-scale wave phase velocity profiles. However, there are two complications. The first is that the factor k_o/k is generally unknown since k is currently unmeasured by JULIA. While it is often the case that k_o/k factor turns out to be close to unity in nature in the daytime, we do not know how universal this ratio is. However, $(1+(k_o/k)^2)^{-1}$ is what we called the α factor in the previous section, where we argued that it can be estimated by calibrating the end result to the 150-km echoes or to seasonal F region averages. (By lumping the ratio of E to F region field strengths into α, E_o can be reinterpreted as the F region zonal electric field.)

The second complication relates to the fact that attempts to model the current density in the equatorial E region by computing the ratio of the conductivities according to (2) historically fail to reproduce *in situ* data (see *Kelley* [1989] and also *Gagnepain et al.* [1977]). The peak in the daytime current density is inevitably predicted to fall at too low an altitude, near 102 km, whereas the true peak height has been measured to be close to 108 km. *Ronchi et al.* [1990] approached the problem with an analysis similar to that of *St.-Maurice* [1987], calculating enhanced electron mobilities and diffusivities associated with the presence of small-scale ($\lambda < 100m$) waves comprising plasma turbulence in the electrojet. By performing a first-order smoothing of the fluid equations, they derived a height-dependent turbulent mobility which can be expressed in the form

$$\sigma_{Pe}^{*} = \frac{1}{2}\frac{\psi}{\psi+1}\left(\frac{\Omega_e}{\nu_e}\right)^2 \left\langle |\delta n/n|^2 \right\rangle \sigma_{Pe} \qquad (4)$$

where $\langle |\delta n/n|^2 \rangle$ is a measure of the intensity of the small-scale electrojet turbulence and is potentially height dependent. The total Pedersen conductivity is the sum of the classical ion, electron, and turbulent electron contributions. Using *in situ* measurements of electrojet density fluctuations taken from *Pfaff et al.* [1987], *Ronchi et al.* [1990] were able to predict current density altitude profiles more consistent with observations.

Our strategy for inferring the zonal electric field from the measured drift profiles makes use of the turbulent mobility correction given by (4). We add this correction to the Pedersen conductivity term in (3) and solve for what remains. The collision frequencies are known quantities; we estimate them using expressions given by *Forbes* [1981] and from neutral temperatures and densities provided by the MSISE90 model. This leaves two free parameters, the turbulent intensity $\langle |\delta n/n|^2 \rangle$ and the zonal electric field term $\alpha E_o/B$, which are taken to be height-invariant constants and fit for in order to minimize the χ^2 error between the data and the model.

Note that we can also generalize the model by assuming a form for the turbulent intensity parameter that decreases exponentially with height. However for the case of the data in Figure 2, best fits were obtained with values of $\langle |\delta n/n|^2 \rangle$ that were essentially constant over E region altitudes.

Summary

In this paper, we have 1) illustrated the capabilities of a new coherent scatter radar system at Jicamarca, 2) outlined a method for estimating the zonal electric field from electrojet interferometry data, and 3) pointed out that the zonal drifts of km-scale waves in the equatorial electrojet appear to be strongly affected by wavelike motion of the neutral atmosphere. The third point has not been reported on widely before, in part because electrojet observations tend to be made for minutes rather than hours at a time at Jicamarca. The dawning of JULIA is timely, since it is only now that the chemical release data from the Guará experiments reveal the unexpectedly complicated neutral wind dynamics in the lower thermosphere.

Acknowledgments.
This work was supported by the National Science Foundation through Cooperative Agreements ATM-9022717 and ATM-9408441 and by NSF Grants ATM-9415931 and ATM-9424550. The Jicamarca Radio Observatory is operated by the Geophysical Institute of Perú, Ministry of Education, with support from the NSF Cooperative Agreements just mentioned. The help of the staff and especially Gabriel Michue was much appreciated.

References

Balsley, B. B., and R. F. Woodman, On the control of the F region drift velocity by the E region electric field: experimental evidence, *J. Atmos. Terr. Phys.*, *31*, 865, 1969.
Farley, D. T., H. M. Ierkic, and B. G. Fejer, Radar interferometry: A new technique for studying plasma turbulence in the ionosphere, *J. Geophys. Res.*, *86*, 1467, 1981.
Fejer, B. G., D. T. Farley, R. F. Woodman, and C. Calderon, Dependence of equatorial F-region vertical drifts on season and solar cycle, *J. Geophys. Res.*, *84*, 5792, 1979.
Forbes, J. M., The equatorial electrojet, *Rev. Geophys.*, *19*, 469, 1981.
Forbes, J. M., and R. S. Lindzen, Atmospheric solar tides and their electrodynamic effects–II. The equatorial electrojet, *J. Atmos. Terr. Phys.*, *38*, 911–920, 1976.
Forbes, J. M., and F. Vial, Monthly simulations of the solar semidiurnal tide in the mesosphere and lower thermosphere, *J. Atmos. Terr. Phys.*, *51*, 649, 1989.
Gagnepain, J., M. Crochet, and A. D. Richmond, Comparison of equatorial electrojet models, *J. Atmos. Terr. Phys.*, *39*, 1119, 1977.
Hagan, M. E., J. M. Forbes, and F. Vial, On modeling migrating solar tides, *Geophys. Res. Lett.*, *22*, 893–896, 1995.
Kelley, M. C., *The Earth's Ionosphere*, Academic, San Diego, Calif., 1989.
Kudeki, E., D. T. Farley, and B. G. Fejer, Long wavelength irregularities in the equatorial electrojet, *Geophys. Res. Lett.*, *9*, 684, 1982.
Kudeki, E., and C. D. Fawcett, High resolution observations of 150 km echoes at Jicamarca, *Geophys. Res. Lett.*, *18*, 1987, 1993.
Kudeki, E., B. G. Fejer, D. T. Farley, and C. Hanuise, The Condor equatorial electrojet campaign: Radar results, *J. Geophys. Res.*, *92*, 13561, 1987.
Larsen, M. F., and C. D. Odom, Observations of altitudinal and latitudinal E-region neutral wind gradients near sunset at the magnetic equator, *Geophys. Res. Lett.*, 1997, this issue.
Pfaff, R. F., M. C. Kelley, E. Kudeki, B. G. Fejer, and K. D. Baker, Electric field and plasma density measurements in the strongly driven daytime equatorial electrojet 2. The unstable layer and gradient drift waves, *J. Geophys. Res.*, *92*, 13,578, 1987.
Ronchi, C., R. N. Sudan, and P. L. Similon, Effect of short-scale turbulence on kilometer wavelength irregularities in the equatorial electrojet, *J. Geophys. Res.*, *95*, 189, 1990.
St.-Maurice, J. P., A unified theory of anomalous resistivity and Joule heating effects in the presence of ionospheric E region irregularities, *J. Geophys. Res.*, *92*, 4533, 1987.
Woodman, R. F., and F. Villanueva, Comparison of electric fields measured at F region heights with 150 km irregularity drift measurements. Proceedings of the Ninth International Symposium on Equatorial Aeronomy, Bali, Indonesia, March 20-24, 1995.

D. L. Hysell and M. F. Larsen, Dept. of Physics and Astronomy, Clemson University, Clemson, SC 29634.
R. F. Woodman, Instituto Geofísico del Perú, Lima.

(received November 13, 1996; revised January 3, 1997; accepted January 23, 1997.)